mining

MDPI

Article

An Advanced Approach for Geometallurgical Modeling Applied to Bauxite Mines

Edmo Rodovalho [1,2,*], José Lima [3], Pedro Campos [1], Pedro Casagrande [1] and Douglas Mazzinghy [1]

[1] Graduate Program in Metallurgical, Materials and Mining Engineering, Universidade Federal de Minas Gerais (UFMG), Belo Horizonte 31270-901, MG, Brazil; pedrocampos@demin.ufmg.br (P.C.); pcasagrande@demin.ufmg.br (P.C.); dmazzinghy@demin.ufmg.br (D.M.)
[2] Institute of Science and Technology, Universidade Federal de Alfenas (UNIFAL), Alfenas 37130-001, MG, Brazil
[3] Mineração Rio do Norte S/A (MRN), Porto Trombetas, Oriximina 68275-000, CEP, Brazil; jose.lima@mrn.com.br
* Correspondence: edmo.rodovalho@unifal-mg.edu.br

Abstract: Geometallurgy is an approach that integrates geology, mining, processing, and environmental areas, aiming to increase knowledge of the deposit and reduce risks in mining projects and/or operations. Growing changes in economic and operational scenarios require the development of robust models for metallurgical responses. Typically, the population of geometallurgical variables is small, and there are restrictions on applying geostatistical techniques, such as Ordinary Kriging, since recoveries are considered non-additive variables. This study used multiple linear regression to develop a geometallurgical model for a bauxite mine. The developed models enabled reconciliation with real results, and this application for bauxite mining represents a novelty in the literature. The model estimated the mass recovery in the coarse fraction with an accuracy greater than 97%. Additionally, the geometallurgical model developed for Mineração Rio do Norte (MRN) allows predictability and mapping potential product quality deviations.

Keywords: multiple linear regression; bauxite; geometallurgy; modeling

Academic Editor: Behnam Sadeghi

Received: 29 November 2024
Revised: 9 January 2025
Accepted: 30 January 2025
Published: 1 February 2025

Citation: Rodovalho, E.; Lima, J.; Campos, P.; Casagrande, P.; Mazzinghy, D. An Advanced Approach for Geometallurgical Modeling Applied to Bauxite Mines. *Mining* **2025**, *5*, 11. https://doi.org/10.3390/mining5010011

1. Introduction

The relationship between mining and society has undergone significant changes in recent decades, with the primary challenge being the integration of this sector into global value chains. While there is a growing demand for various metals to support new large-scale consumption habits, this does not imply that mining should be carried out at any cost. Society's demands are spread in the social, economic, and environmental spheres, but currently, there is a need for advances in process predictability and waste management in mining [1,2]. The mining industry is required to process materials at increasingly lower grades and develop mining areas with complex geology [3]. To control these risks, many mining sites have invested in geometallurgy.

Geometallurgy is a multidisciplinary approach to the mining production process that aims to integrate all elements within a given mineral value chain [4]. For each metallic substance, the mineral value chain has a different set of processes (links), with its core consisting of mineral resource estimation, reserve evaluation, and mining sequencing [5]. On one side lies geological exploration and modeling, while on the other are metallurgical processes. Effective risk management, waste management, cost control, and predictability of the performance of metallurgical processes require communication and exchange of information between the ends of this chain [6,7].

The geometallurgical model seeks to map the spatial variability of material behavior during mineral processing [8]. To obtain a product with a determined quality specification, it is necessary to process different types of materials, which can be measured by some variables, such as energy consumption, reagent consumption, and mass recovery [9]. In addition to the grade and density variables provided by geological models, geometallurgical models incorporate spatial estimates of mass recovery and other mineral processing variables. However, the limited number of geometallurgical variables, such as the comminution index and recoveries, renders geostatistical techniques like Ordinary Kriging unsuitable for estimation [8]. Other challenges in estimating geometallurgical variables are associated with the non-additive behavior of these variables, the support of the estimation, and ore blending [10,11].

There are no publications that describe the estimation of geometallurgical variables regarding large bauxite mining operations. The description of a geometallurgical program for tabular bauxite deposits is also an unprecedented topic in the scientific literature. A related study focuses on MRN bauxite operations, describing investigations to optimize production planning through geometallurgical models [12]. A recent study describes case studies for metallic deposits but with different genesis and geological processes [13]. The processes of metamorphism, weathering, and mineralogical controls influence the segregation of geometallurgical domains. Consequently, methods for estimating geometallurgical variables are applied to data within these domains. Considering mineralogical analysis, a study used XRD analysis to classify bauxite samples, linking mineralogical composition with processing performance [14]. Another study applied techniques for updating geometallurgical models in bauxite deposits using compositional data [15]. As there are still no publications describing a case study of geometallurgy applied to bauxite mining, the present work seeks to answer the following research question: How does one estimate mass recovery variables for bauxite deposits?

The present work seeks to describe a case study of a large bauxite mine located in Brazil that developed a geometallurgical program. The objective is to outline the procedures necessary to create a geometallurgical model for a bauxite mine and evaluate its effectiveness. Key aspects of the discussion include the methods for estimating geometallurgical variables, validation, reconciliation, and model implementation. Exploratory data analysis and the segregation of geometallurgical domains are also addressed

The dataset, obtained through drill hole sampling, includes variables typically relevant to bauxite, such as usable alumina (ALAP), reactive silica (SIRE), and other contaminants segregated by particle size ranges. Additionally, mass recovery results are available for the coarse fraction. All variables are regionalized and georeferenced within the bauxite plateaus analyzed in this study.

2. Methodology

The geometallurgy program hereby analyzed aimed to develop a geometallurgical model capable of reliably predicting variations in mass recovery in mineral processing. The bauxite processing unit involved in this case study primarily consisted of crushing and particle size classification stages. Products were segregated based on particle size. Therefore, the retained material in the coarse fraction (RECG) and that retained in the fine fraction (RECF) were the main variables that measured the performance of mineral processing, as they directly corresponded to mass recovery.

The mine unit had multiple mining fronts, with different mineralogical and petrological characteristics. It consisted of a tabular bauxite deposit with capping thickness varying from 5 to 10 m, with strip mining being the most suitable mining method [16]. Figure 1

shows 2D contouring of the three plateaus in operation, each containing several mining fronts. All these mining faces fed a primary crushing unit.

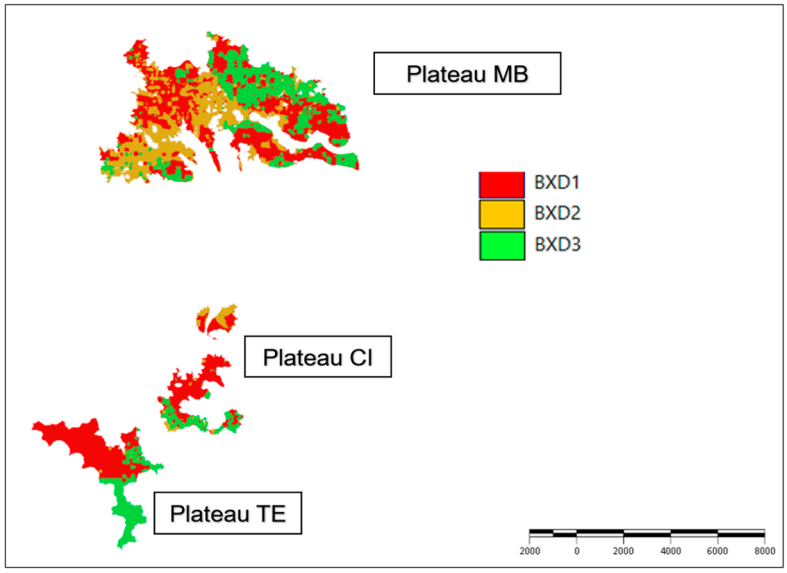

Figure 1. Mining areas with geochemical classification (2D contouring).

Figure 1 presents an initial granulometric/geochemical classification to guide exploratory data analysis. The classification considers the contents of alumina, silica, and iron oxide. Petrological characteristics, such as texture, are also considered to define the solid colors for BXD1, BXD2, and BXD3. The region dominated by alumina-rich minerals is represented by the red color, BXD1. The region with a higher concentration of silica is defined by the orange color, BXD2. Lastly, the region characterized by ferruginous minerals is represented by the green color, BXD3. Figure 2 illustrates the 2D positions of each sample used in this study. The drilling holes had a depth of 20 m, and the grid spacing was 200 m $\times$ 200 m for the TE and MB plateaus. For the CI plateau, the grid spacing was reduced to 100 m $\times$ 100 m in the central region.

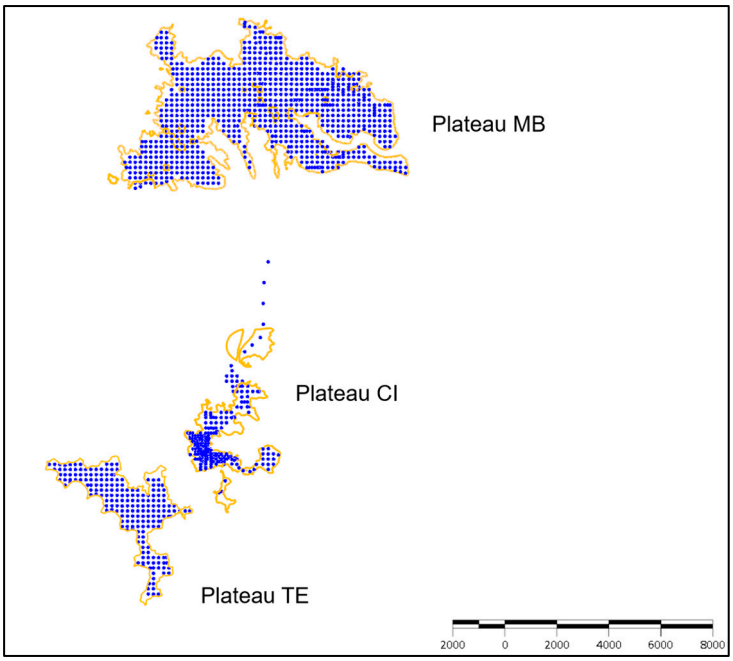

Figure 2. Drill holes' spatial distribution.

Due to the complexity and diversity of materials feeding the mineral processing unit, it was essential to develop a specific geometallurgy program for the studied mine. Addressing this gap enabled the evaluation of the impact of geological variability on process feed performance. The main gaps identified in this study were the following: (1) conducting basic geometallurgical tests to capture variability in the process, such as sieving tests to measure the material retained in each granulometric range; (2) defining geometallurgical domains through exploratory data analysis; (3) generating multivariate models; (4) estimating coarse recovery using multivariate linear regression to populate the block model, due to the need to reach a deterministic equation; and (5) developing a mine plan based on the geometallurgical model and reconciling coarse recovery values (actual versus estimated).

2.1. Exploratory Data Analysis for Population Segregation

For each plateau presented in Figure 1, a drilling hole database was available, containing variables such as grades, retained material in the fine and coarse fractions, densities, moisture content, and geological/size chemical classifications. Table 1 provides a description of each variable analyzed in this study. This list summarizes all the available variables to be evaluated using multivariate linear regression methods.

Table 1. Description of the variables for the studied mine's dataset.

Variables	Type	Description
LITO	Numeric	Lithology code
LITOREV	Text	Lithology domain (BXD1, BXD2 and BXD3)
DENSITY	Numeric	Density
DENSU	Numeric	Wet density
DENSS	Numeric	Dry density
UMID	Numeric	Moisture
RECG	Numeric	Mass of coarse fraction after screening
ALTG	Numeric	Total alumina content (grade) in the coarse fraction
SITG	Numeric	Total silica content (grade) in the coarse fraction
FETG	Numeric	Total iron content (grade) in the coarse fraction
TITG	Numeric	Total titanium content (grade) in the coarse fraction
PPCG	Numeric	Calcination grade in the coarse fraction
ALAPG	Numeric	Alumina content (grade) in the coarse fraction
SIRG	Numeric	Reactive silica content (grade) in the coarse fraction
RECF	Numeric	Mass of fine fraction after screening
ALTF	Numeric	Total alumina content (grade) in the fine fraction
SITF	Numeric	Total silica content (grade) in the fine fraction
FETF	Numeric	Total iron content (grade) in the fine fraction
TITF	Numeric	Total titanium content (grade) in the fine fraction
PPCF	Numeric	Calcination grade in the fine fraction
ALAPF	Numeric	Alumina content (grade) in the fine fraction
SIRF	Numeric	Reactive silica content (grade) in the fine fraction

The primary objective of this step was to define the geometallurgical domains based on the statistical behavior of the RECG and RECF variables.

The first step involved analyzing histograms for the RECG and RECF variables within each of the geological model sections: BXD1, BXD2, and BXD3. Figure 3 presents these histograms side by side, allowing for a graphical evaluation of the differences in the mean and standard deviation of each variable.

The histograms reveal a significant deviation in the BXD2 population compared to the combined BXD1 and BXD3 populations. The three histograms on the right side, which correspond to the coarse fraction, show a higher percentage of material retained. However,

the BXD2 model exhibits a significantly lower average of retained percentage compared to the broader data population.

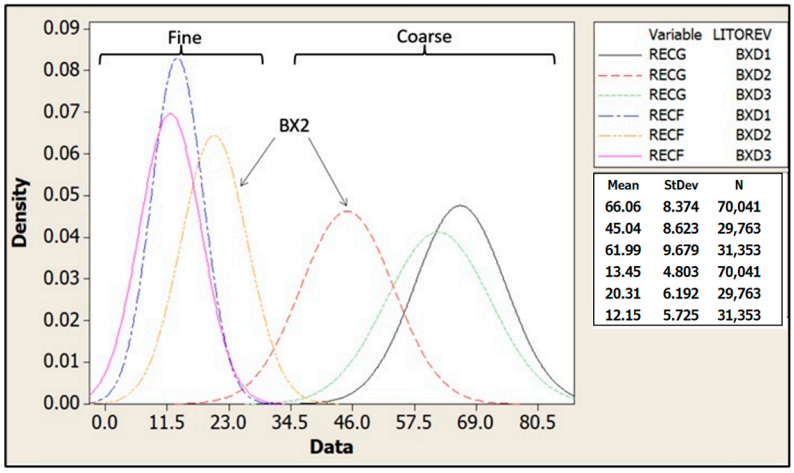

Figure 3. Histograms for fine and coarse fractions (TE plateau).

Similarly, deviations are observed in the fine fraction, suggesting that the BXD1 and BXD3 populations exhibit similar behavior during sieving. This indicates that higher mass recovery in the coarse fraction can be expected when the plant is fed with material from BXD1 and BXD3.

The graph in Figure 3 corresponds to the TE plateau and was reproduced for the CI and MB plateaus. In all these mining areas, the same behavior described in Figure 3 was observed. Following the identification of this behavior, it became necessary to analyze boxplot graphs to further evaluate the differences between the BXD2 population and the combined BXD1 + BXD3 populations.

Figure 4 presents a boxplot graph that segregates the data populations as follows: samples contained in BXD1 and BXD3 are grouped and classified as GMD1, while samples in BXD2 are classified as GMD2. This graph evaluates the RECG and RECF variables for the TE plateau.

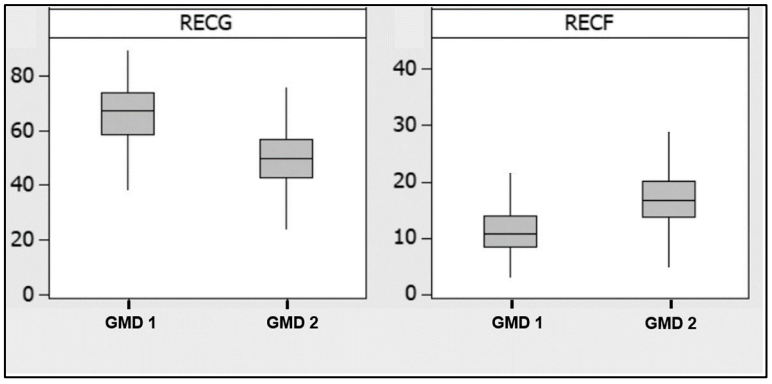

Figure 4. Boxplot of GMD 1 and GMD 2 populations (TE plateau).

Analyzing the boxplots reveals that the dispersions of the two populations are similar. However, a noticeable shift in the medians can be observed across all fractions.

The behavior shown in Figure 4 could be consistently observed across all three mining areas presented in Figure 1. Consequently, it was necessary to test the hypothesis that two geometallurgical domains, GMD1 and GMD2, existed.

The first step involved conducting a normality test, where the P-value for GMD1 and GMD2 in all plateaus was found to be less than 0.005. This result indicated that the

analyzed populations did not follow a normal distribution. Therefore, non-parametric tests were required to evaluate whether the differences between GMD1 and GMD2 were significant with respect to the mass recovery [16].

Using the Kruskal–Wallis test, the P-value was determined to be less than 5% across all fractions and mining areas. This result led to the rejection of the null hypothesis (H°), which posited an insignificant variability between the domains. As a result, the exploratory data analysis (EDA) confirmed that mass recovery exhibited significant variability between the GMD1 and GMD2 geometallurgical domains.

2.2. Definition and Validation of Geometallurgical Domains

Since the GMD1 and GMD2 populations represented distinct groups, it was necessary to perform 3D modeling to generate solids that corresponded to them. The method used to obtain these solids was implicit modeling via the Radial Basis Function (RBF) in Micromine 2024 (mine planning software). This method considers the geological context of each database so that the positions of contacts and the resulting solids are maximally correlated with field observations (such as mapping, geological exploration, and regionalized secondary variables). The most common configurations involve the presence of intrusions, veins, or structural controls. When such entities are present, the method for processing the system of linear equations is adjusted accordingly [13]. Each approach aims to generate solids that are compatible with the geological context of the area. The results are integrated into a 3D block model, with Micromine providing all the necessary tools within the same application. Based on these features, Micromine was selected for use in the present study.

In the context of the current study, no intrusions, veins, or significant structural controls (such as fault planes, discontinuities, or folds) were present. Figure 5 illustrates the 2D contouring of each plateau, which is formed by depositional planes according to the region's stratigraphic sequence. Based on this information, depositional controls were chosen as the basis for the implicit modeling runs. This approach was applied to all other plateaus in the studied mine.

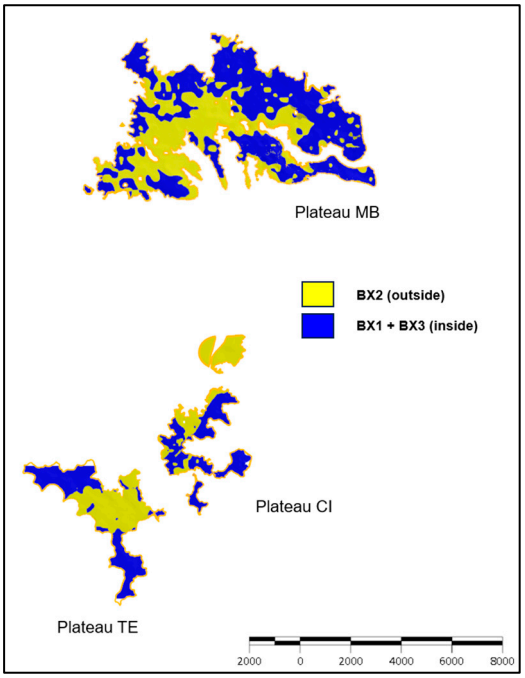

Figure 5. Modeling of the GMD1 and GMD 2 geometallurgical domains.

To validate the results obtained during implicit modeling and test the contacts of the geometallurgical domains, contact analysis was applied to all domains. This method considers the number of samples contained in each solid, the distance to the contact surface, and the variation in content depending on the distance. The results of this analysis can classify contacts as abrupt or soft. Figure 6a presents a contact analysis for the TE plateau. Figure 6b shows a contact analysis for the CI plateau. Figure 6c presents a contact analysis for the MB plateau. All analyses included an analysis of the RECG variable. The results of the graphical analyses indicated hard contact where the recovery variation was abrupt at the boundary between the domains analyzed. This behavior indicated that the geometallurgical model was valid and capable of satisfactorily segregating the populations.

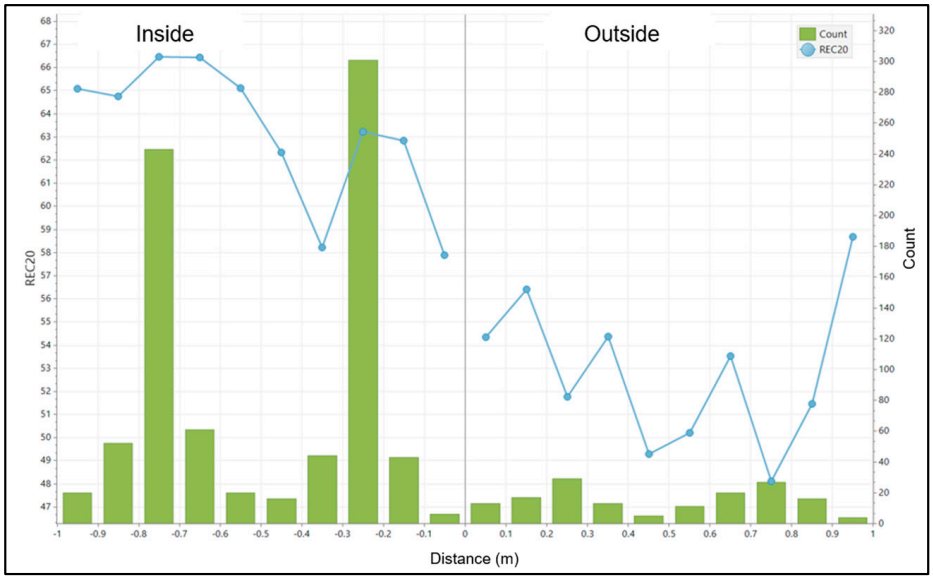

(**a**)

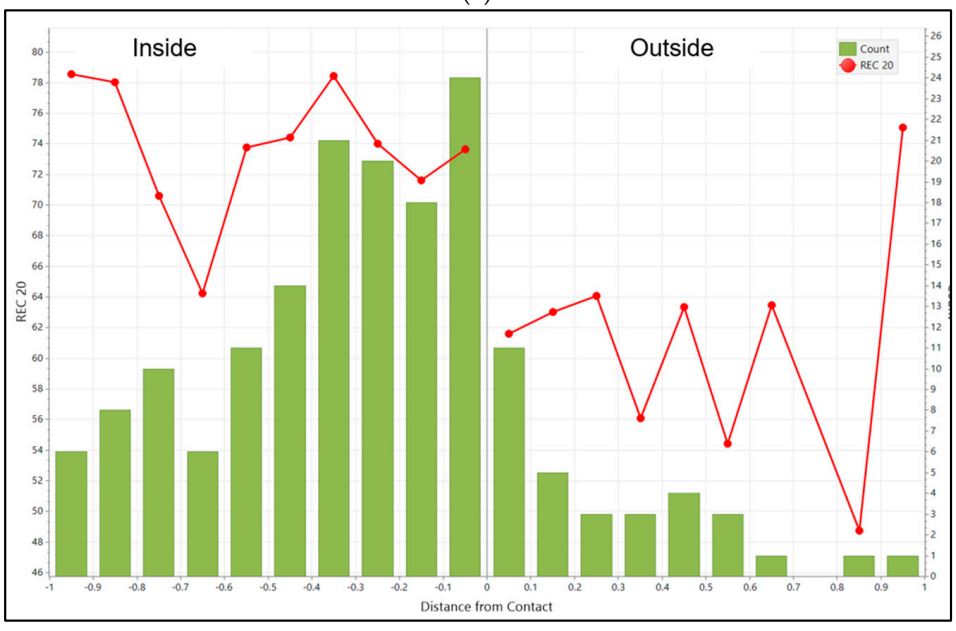

(**b**)

Figure 6. *Cont.*

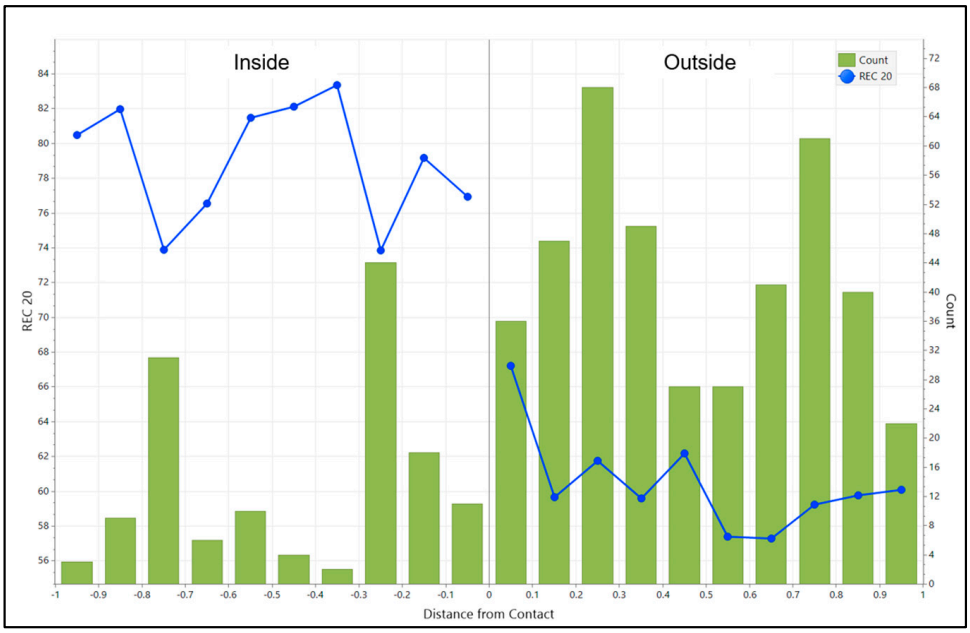

(**c**)

Figure 6. Contact analysis for the geometallurgical domains GMD1 and GMD 2: (**a**) TE plateau, (**b**) CI plateau, and (**c**) MB plateau.

2.3. Variable Selection

The variable selection process began with the application of the correlation matrix, where all physical and chemical variables present in the database and their correlations for each domain, fraction, and plateau were evaluated. Figure 7 presents the correlation matrix of the TE plateau, GMD1, in the coarse fraction. The matrix measured the relationship between the database variables and RECG. The variables with the highest correlation were selected to be analyzed by stepwise regression.

	RECG	UMID	TITG	FETG	ALAPG	SIRG	PPCG
UMID	-0,778 0,000						
TITG	0,067 0,001	-0,328 0,000					
FETG	-0,680 0,000	0,584 0,000	0,088 0,000				
ALAPG	0,121 0,000	0,170 0,000	-0,946 0,000	-0,335 0,000			
SIRG	0,425 0,000	-0,326 0,000	0,171 0,000	-0,305 0,000	-0,117 0,000		
PPCG	0,092 0,000	-0,383 0,000	0,819 0,000	-0,056 0,000	-0,850 0,000	0,174 0,000	
SITG	-0,570 0,000	0,526 0,000	0,161 0,000	0,869 0,000	-0,379 0,000	-0,098 0,000	0,028 0,000

Cell contents: Pearson Correlation
P-Value

Figure 7. Correlation matrix for RECG/GMD1/TE plateau.

Given the large number of variables involved in the process and the long data collection period, it was necessary to use a statistical analysis tool. Minitab16 software was selected for this purpose. This software can select variables according to the level of significance and was used for modeling the investigated scenarios. As the focus of the research was mass recovery in the coarse fraction, this variable was called the response variable, and all other variables were called predictors. To select the predictor variables, the stepwise regression method (forward and backward) was applied, where the analysis started using all variables and then they were successively excluded in increasing order of correlation. Selection was completed when a satisfactory correlation equation was achieved. This method is suitable when many predictor variables have some level of correlation with the response variable. Only the coarse fraction had enough information to build a consistent model. As a result, subsequent analyses did not consider the fine fraction.

Table 2 presents the results of applying the variable selection technique using the stepwise regression method. This corresponded to the coarse fraction of GMD1 on the TE plateau. In step 5, only variables with *p*-values less than 0.15 were selected by the tool. With the evaluation of this parameter in each round, step 5 was the final model of the stepwise regression. Thus, all variables with compatible *p*-values were provided in the model. Table 2 presents the values of the adjusted coefficient of determination (R2 adj), which is useful for comparing models with different numbers of predictors. The higher the R2 adj value, the better the model fits the data. The same technique was applied to all plateaus and domains of the studied mine.

Table 2. Stepwise regression for plateau TE/GMD 1/RECG.

Response	**Mass Recovery**				
Step	1	2	3	4	5
Constant	89.1	91.2	1508.9	−1384	84.9
Variables			**Coefficients**		
UMID	−1.9	−2.7	−2.3	−2.82	−2.85
TITG		7.1	7.91	8.15	8.09
FETG			0.45	0.47	0.44
ALPG				−0.04	−0.05
SIRG					−0.97
R^2_{ADJ}	75.1	76.5	82.3	83.1	85.2

2.4. Model Development and Validation

Considering the results presented in Table 2, step 5 presented the parameters that best explained the mass recovery in the coarse fraction (TE Plateau/GMD1), using Equation (1). The next step was to conduct a residual portion analysis. Specifically, it was necessary to check the presence of autocorrelation in the residuals from the regression. Durbin–Watson statistics and Cook's distance analysis were the most efficient tools for this analysis. In Equation (1), the value of the Durbin–Watson statistic obtained was equal to 1.25, indicating that the residuals were independent, and there was no autocorrelation. The analysis of Cook distances did not indicate any influential points. Both analyses showed the consistency of the model that described mass recovery in the coarse fraction (plateau TE/GMD1).

$$RECG = 84.9 - 2.85 \times [UMID] + 8.09 \times [TITG] + 0.441 \times [FETG] - 0.0475 \times [ALAPG] - 0.970 \times [SIRG] \quad (1)$$

For additional validation of the model, a graphical residual analysis was performed. For this routine, it was necessary to ensure that the residuals followed a normal distribution, had constant variance, and were independent, as assumed in a multiple linear regression model. In Figure 8a, the normal probability plot shows that the points follow the theoretical

normal probability line, with *p*-values >0.15; therefore, it can be assumed that the residuals do not deviate significantly from a normal distribution. Figure 8b shows the plot of residuals versus the fitted values, where the assumption of constant variance is not violated. The residuals are randomly distributed around zero and have approximately the same dispersion for all fitted values. No outliers are present. Figure 8c presents the graph of residuals versus the order of observation; the points do not show a trend and, therefore, it is assumed that the errors are independent. In Figure 8d, the histogram presents information compatible with a normal distribution. Thus, all elements necessary to validate the model were satisfactorily fulfilled. Therefore, Equation (1) can adequately explain the mass recovery in the coarse fraction (TE plateau/GMD1).

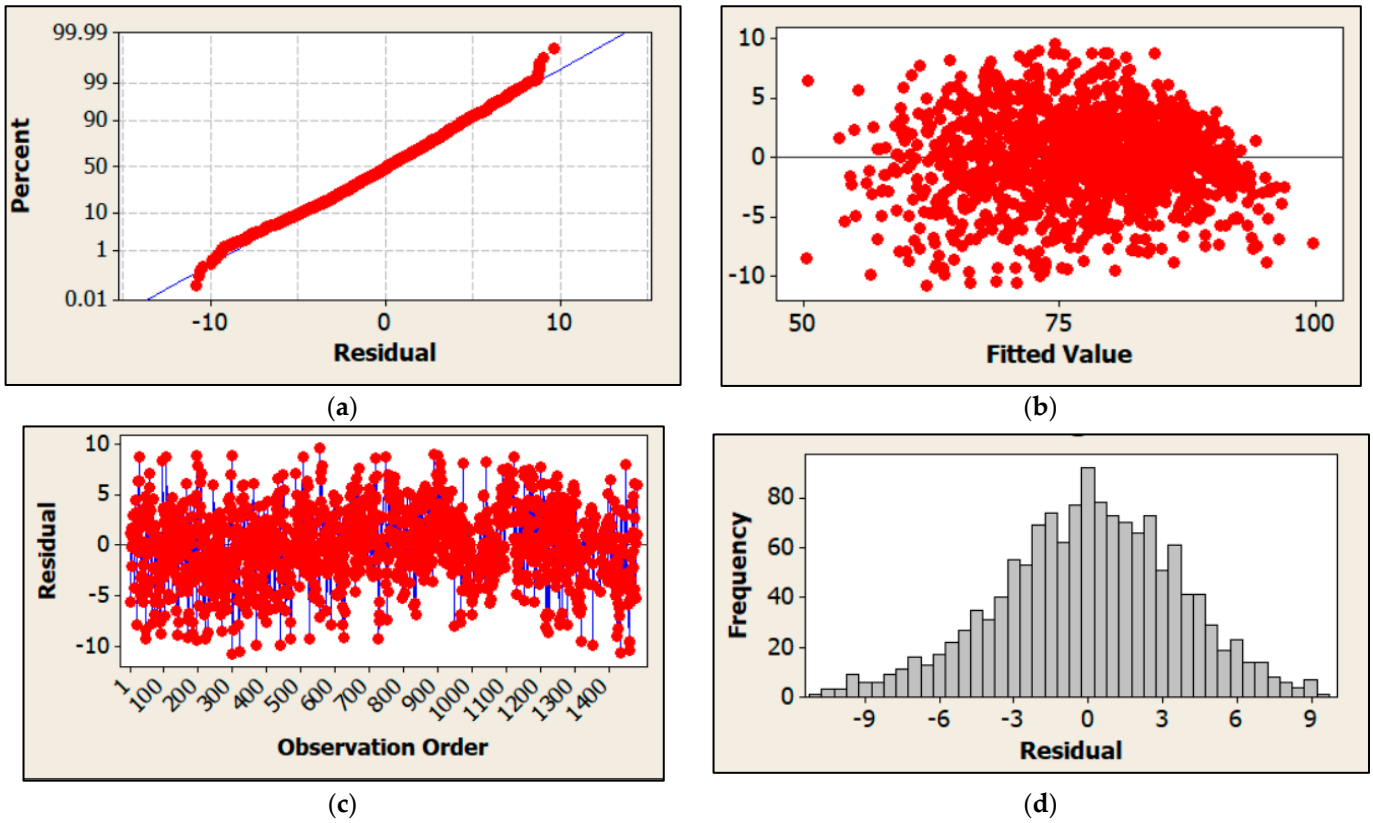

Figure 8. Residual analysis: (**a**) residual normality check chart for RECG/GMD1/TE plateau; (**b**) residual evaluation graph versus adjusted RECG/GMD1/TE plateau values; (**c**) graph of residuals (red) versus observations (blue line)RECG/GMD1/TE plateau; and (**d**) histogram analysis of RECG/GMD1/TE plateau residues.

3. Practical Application

The procedures described in the previous section were applied to all plateaus in Figure 1. As a result, one model was developed for each fraction, domain, and plateau, totaling twelve models. These multivariate linear regressions were implemented in the block model to estimate the RECG and REC values that compose the geometallurgical model of the studied mine. Figure 9 summarizes the practical application procedure, which begins with the generation of multivariate linear regression models (MLRM—step 1), followed by the estimation of the retained RECF and RECG values. From phase 3 onwards, the operational approach takes place, with practical application in an active mine. Mine planning was developed using the geometallurgical model, and the estimated results were compared with those performed by a mineral processing unit. This procedure was called

reconciliation and is provided below for step 4 of the method of the practical application of the geometallurgy program.

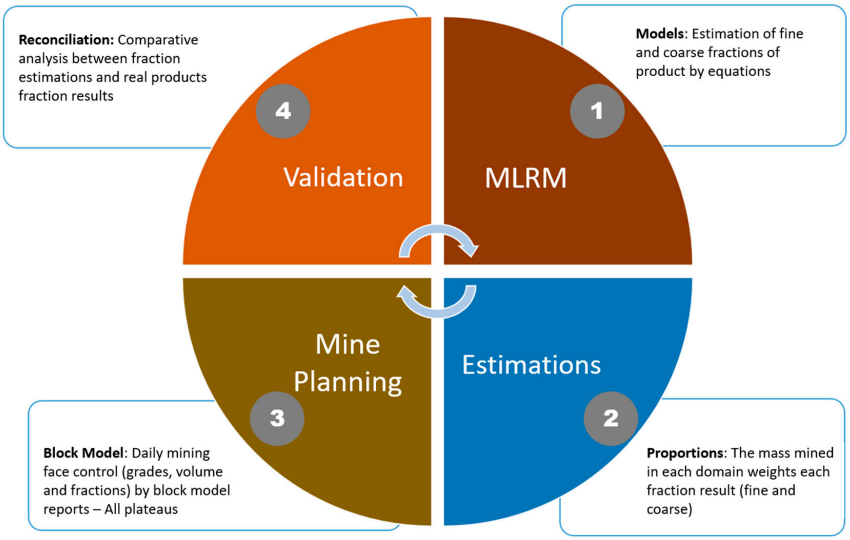

Figure 9. Methodology for the practical application of the geometallurgical model.

Figure 10 presents the results of the estimates for the MB, TE, and CI plateaus by 2D contouring, where the cold colors indicate the lowest mass recoveries for the coarse fraction and the warm colors indicate the highest values. The blending of these three mining areas constitutes the feed for the mineral processing unit.

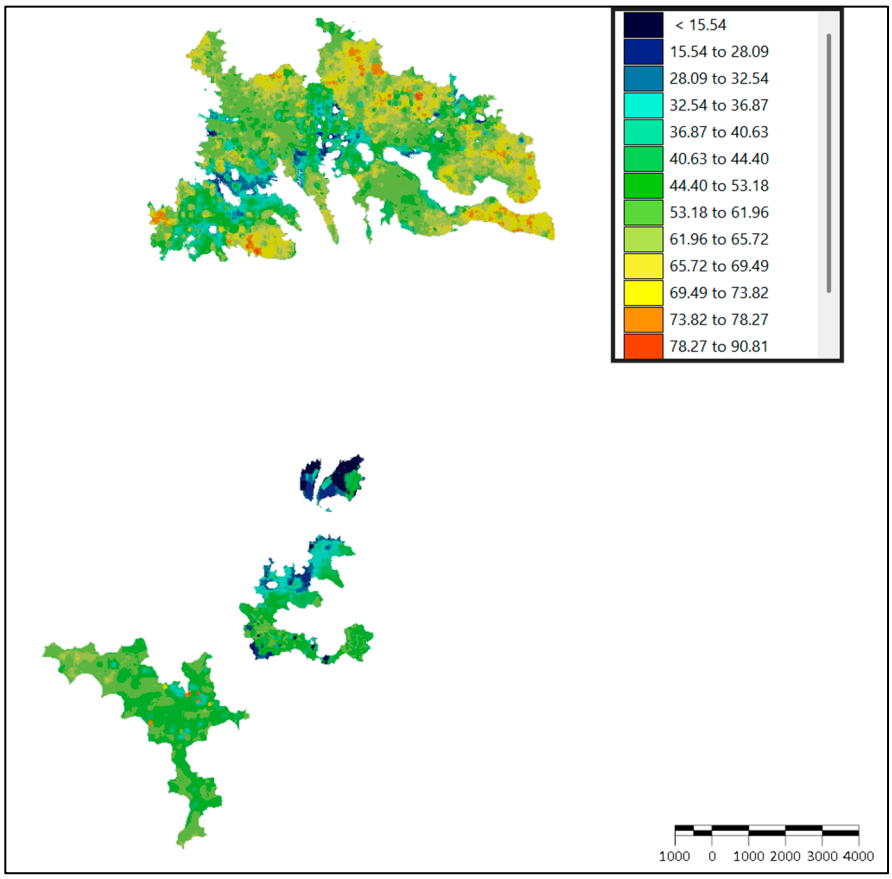

Figure 10. Estimated geometallurgical models (2D contouring).

4. Results and Discussions

The geometallurgical model was used to develop a short-term plan in the studied mine to validate and measure the effectiveness of the model. Although estimated results were available for all fractions, this work focused on validating the model only for the coarse fraction. This was due to operational limitations of the mine studied to evaluate the fine fraction. It is important to emphasize that the limitations of the processing unit do not affect the validation and reconciliation of the model. Additionally, it is worth noting that the objective of this work is to evaluate the model's efficiency for any fraction.

The statistical validation procedures to verify the practical applicability of the models were successfully conducted. The results presented in Table 2 indicate a high correlation index, which implies the high capacity of the models to explain the mass recovery variable. Furthermore, the errors maintained the statistical behavior in both subpopulations, which indicates the validity of the model and the ability to replicate the same results without any bias. As the present study considers three mining areas, it is important to highlight that the results presented and discussed in Figure 8a–d also apply to the MB and CI plateaus. Table 3 presents the mass recovery results for the coarse fraction, based on tests conducted over four weeks and involving all mining areas (MB, CI, and TE).

Table 3. Coarse bauxite processing results after the geometallurgical approach.

Coarse Mass Recovery Results	
Real	66.2%
Estimation	67.8%
Variation	2.4%

The results obtained after applying the geometallurgical model estimated via multivariate linear regression confirm the validity and the ability to generate mineral processing performance predictions. Despite requiring a long period of data analysis, the application of the geometallurgical model does not require an adaptation period in the mineral processing unit or mining operations. Over the four weeks of testing, mining operations alternated between plateaus, with only two of the three plateaus participating in the feed at a time. This alternation is a common characteristic of the mining process and highlights the importance of testing over several weeks to avoid bias from this practice. Despite this, the results showed only a 2.4% deviation between the estimated and actual mass recovery for the coarse fraction. Based on previous studies, this value can be considered a low deviation for geometallurgical models [11]. This outcome concludes the validation and reconciliation phase of the model, demonstrating its capability to make reliable predictions. While only the coarse fraction was modeled due to operational constraints, the studied mine plans to gradually incorporate fine fraction data using predictive methods and estimation tools.

5. Conclusions

The application of statistical analysis tools and modeling techniques via multivariate linear regression has proven to be an effective alternative in the development of geometallurgy programs. The model developed successfully identified the variables that are most relevant to mineral processing and prioritized them accordingly. This result optimizes resources and efforts to avoid deviations and losses in processing. This method offers an important contribution in an economic environment where control and predictability of operational variables become fundamental for organizations to remain in the global aluminum market. The mass recovery of the coarse fraction from bauxite processing was estimated with high accuracy, and the objective of this study was achieved with model

validation. Furthermore, implementing this method in routine mining operations, using existing resources and without requiring large investments, represents a significant advancement for the industry.

Among the results achieved is the compatibility between the geometallurgical model and the bauxite processing plant, with an accuracy greater than 97% for the coarse fraction. In addition to this important result, the present study validated the application of multivariate linear regression in estimating geometallurgical models in bauxite mining. Both findings are unprecedented in the bauxite mining industry and the literature. The method proved to be valid and applicable to other mining enterprises of all sizes, as it is a suitable tool for identifying relevant variables and prioritizing critical points in geometallurgy programs. The basic requirement for implementing this model in other mines is the availability of data for modeling. Furthermore, each mine has a group of variables with greater influence on metallurgical responses.

Complementing this research, a regular re-evaluation of such results is necessary to verify the behavior of the variables in relation to variations in grades in the mining areas. Further studies will extend validation to include longer-term and seasonal performance data. In addition, the availability of more information on the fine fraction will allow a more comprehensive approach. The variability in grades in the studied mine and other similar units is significant. New estimation methods can be applied to this same dataset, such as random forest and machine learning techniques. These methods can improve the model's accuracy and provide an easier mine planning approach. Another area for further evaluation is the reduction in test times, which would enable short-term analyses. This approach could help assess potential seasonal fluctuations in performance. The goal of these future studies is to improve the predictability of metallurgical responses, leading to increased productivity, energy efficiency, safety, and better environmental performance. As part of further educational efforts, a synthetic dataset for bauxite geometallurgical modeling will be developed.

Author Contributions: Conceptualization, E.R. and J.L.; methodology, E.R and D.M.; statistical software, P.C. (Pedro Campos); geological modeling software, E.R and P.C. (Pedro Casagrande); formal analysis, E.R. and J.L.; investigation, E.R.; writing—original draft preparation, E.R. and J.L.; writing—review and editing, P.C. (Pedro Campos); visualization, P.C. (Pedro Casagrande); supervision, D.M.; project administration, D.M.; and funding acquisition, J.L. All authors have read and agreed to the published version of the manuscript.

Funding: This research was funded by Mineração Rio do Norte (MRN), grant number CT3416.

Data Availability Statement: Data are not available publicly due to confidentiality reasons.

Acknowledgments: The authors would like to thank Mineração Rio do Norte (MRN) for the funding and research support and MICROMINE for the technical support.

Conflicts of Interest: The authors declare that this research was conducted in the absence of any commercial or financial relationships that could be construed as potential conflicts of interest.

References

1. Jupp, K.; Howard, T.J.; Everett, J.E. Generating synthetic data for simulation modeling in iron ore. *Min. Technol.* **2014**, *123*, 39–46. [CrossRef]
2. Bridge, R.; Brosig, D.; Lozano, C.; Laurila, H. Geometallurgy: An underutilized technology. *Can. Inst. Min. Metall. Pet.* **2014**, *23*, 81–87.
3. Lishchuk, V.; Pettersson, M. The mechanisms of decision-making when applying geometallurgical approach to the mining industry. *Miner. Econ.* **2021**, *34*, 71–80. [CrossRef]
4. Madenova, Y.; Madani, N. Application of Gaussian Mixture Model and Geostatistical Co-simulation for Resource Modeling of Geometallurgical Variables. *Nat. Resour. Res.* **2021**, *30*, 1199–1228. [CrossRef]

5. Del Castillo, M.F.; Dimitrakopoulos, R. A multivariate destination policy for geometallurgical variables in mineral value chains using coalition-formation clustering. *Resour. Policy* **2016**, *50*, 322–332. [CrossRef]
6. Dominy, S.C.; O'Connor, L.; Parbhakar-Fox, A.; Glass, H.J.; Purevgerel, S. Geometallurgy—A Route to More Resilient Mine Operations. *Minerals* **2018**, *8*, 560. [CrossRef]
7. Navarra, A.; Grammatikopoulos, T.; Waters, K. Incorporation of geometallurgical modelling into long-term production planning. *Min. Eng.* **2018**, *120*, 118–126. [CrossRef]
8. Hoffmann, J.; Augusto, J.; Resende, L.; Mathias, M.; Mazzinghy, D.; Bianchetti, M.; Mendes, M.; Souza, T.; Andrade, V.; Domingues, T.; et al. Modeling Geospatial Uncertainty of Geometallurgical Variables with Bayesian Models and Hilbert–Kriging. *Math Geosci.* **2022**, *54*, 1227–1253. [CrossRef]
9. Boisvert, J.B.; Rossi, M.E.; Ehrig, K.; Deutsch, C.V. Geometallurgical Modeling at Olympic Dam Mine, South Australia. *Math. Geosci.* **2013**, *45*, 901–925. [CrossRef]
10. Campos, P.H.; Costa, J.F.; Koppe, V.C.; Bassani, M.; Deutsch, C. Short-Term Schedule Optimization with Nonlinear Blending Models for Improved Metallurgical Recovery in Mining. *Min. Metall. Explor.* **2024**, *41*, 1629–1643. [CrossRef]
11. Lishchuk, V.; Koch, P.H.; Ghorbani, Y.; Butcher, A.R. Towards integrated geometallurgical approach: Critical review of current practices and future trends. *Miner. Eng.* **2020**, *145*, 106072. [CrossRef]
12. Martins, M.A.S.; Medeiros, H.; Dos Santos, B.Y.B. Geometallurgical Studies for the Mineração Rio Do Norte Bauxites Plateau Saracá III, Brazil. In Proceedings of the Society for Mining, Metallurgy & Exploration, Englewood, CO, USA, 1998; SME: Englewood, CO, USA, 1998.
13. Beaumont, C.; Musingwini, C. Application of geometallurgical modelling to mine planning in a copper-gold mining operation for improving ore quality and mineral processing efficiency. *J. S. Afr. Inst. Min. Metall.* **2019**, *119*, 243–252. [CrossRef]
14. Antoniassi, J.L.; Kahn, H.; Ulsen, C.; Tassinari, M.M.M.L. Prediction of Mineral Processing Behavior of Bauxite Ores by XRD Cluster Analysis. In Proceedings of the 10th International Congress for Applied Mineralogy (ICAM), Trondheim, Norway, 1–5 August 2012; Broekmans, M., Ed.; Springer: Berlin, Heidelberg, 2012. [CrossRef]
15. Prior, Á.; Tolosana-Delgado, R.; van den Boogaart, K.G.; Benndorf, J. Resource Model Updating for Compositional Geometallurgical Variables. *Math. Geosci.* **2021**, *53*, 945–968. [CrossRef]
16. Montgomery, D.C.; Runger, G.C. *Applied Statistics and Probability for Engineers*, 4th ed.; John Wiley & Sons: Phoenix, AZ, USA, 2007.